

## Author's Accepted Manuscript

The similar *in-situ* polymerization of nano cupric oxide preparation and phenol formaldehyde resin synthesis: The process and mechanism

Tengfei Yi, Sisi Zhao, Wei Gao, Congnan Guo,  
Long Yang, Guanben Du



PII: S0143-7496(18)30233-1  
DOI: <https://doi.org/10.1016/j.ijadhadh.2018.10.003>  
Reference: JAAD2274

To appear in: *International Journal of Adhesion and Adhesives*  
Accepted date: 1 October 2018

Cite this article as: Tengfei Yi, Sisi Zhao, Wei Gao, Congnan Guo, Long Yang and Guanben Du, The similar *in-situ* polymerization of nano cupric oxide preparation and phenol formaldehyde resin synthesis: The process and mechanism, *International Journal of Adhesion and Adhesives*, <https://doi.org/10.1016/j.ijadhadh.2018.10.003>

This is a PDF file of an unedited manuscript that has been accepted for publication. As a service to our customers we are providing this early version of the manuscript. The manuscript will undergo copyediting, typesetting, and review of the resulting galley proof before it is published in its final citable form. Please note that during the production process errors may be discovered which could affect the content, and all legal disclaimers that apply to the journal pertain.

# The similar *in-situ* polymerization of nano cupric oxide preparation and phenol formaldehyde resin synthesis: The process and mechanism

Tengfei Yi<sup>a, b, c</sup>, Sisi Zhao<sup>a, b, c</sup>, Wei Gao<sup>a, b, c\*</sup>, Congnan Guo<sup>a, b, c</sup>, Long Yang<sup>a, b, c</sup>, Guanben Du<sup>a, b, c</sup>

<sup>a</sup> Key Laboratory for Forest Resources Conservation and Utilization in the Southwest Mountains of China (Southwest Forestry University), Ministry of Education, Kunming, Yunnan Province 650224, People's Republic of China

<sup>b</sup> Yunnan Key Laboratory of Wood Adhesives and Glue Products, Southwest Forestry University, Kunming, Yunnan Province 650224, People's Republic of China

<sup>c</sup> College of Material Science and Engineering, Southwest Forestry University, Kunming, Yunnan Province 650224, People's Republic of China

\* Correspondence author: Wei Gao (E-mail: weigaoe@gmail.com)

## Abstract

The process and mechanism of phenol-formaldehyde (PF) resin synthesis and nano copper oxide (CuO) preparation simultaneously in the same reaction vessel were studied in this paper. Curing kinetics, molecular structure changes as well as the bonding performance of the modified PF resin was investigated. The results indicated that loading levels of the derived nano CuO at 4% and 8% reduced the apparent activation energy of the PF resin and accelerated both the addition and condensation reactions, while changes of reaction enthalpy were consistent of these results. With the introduction of the derived nano CuO, the chemical shifts of all samples were generally offset to the low field for the solvent effect. A complexation reaction between copper ions and

oxygen on the phenolic hydroxyl groups had an influence on phenoxy carbons as shown by NMR. Quantitative analysis indicated that nano CuO had a positive effect on *para* substituted reaction and thus enhanced both the addition and the condensation reactions. Though the shear strength under several test conditions decreased slightly, values were within the requirements set by the appropriate Chinese Standard.

### Keywords

phenol-formaldehyde resin; nanometer copper oxide; differential scanning calorimetry (DSC);  $^{13}\text{C}$  nuclear magnetic resonance ( $^{13}\text{C}$  NMR with CP-MAS); plywood

## 1. Introduction

A PF resin is the polycondensation product of the reaction of phenol with formaldehyde [1]. It was the first thermosetting resin synthesized, this being in 1907, and PF resins have since been shown to possess many good properties including resistance to heat, corrosion, wear, and excellent adhesive-related capabilities [2]. Nowadays, PF resins are still widely applied in the manufacture of wood-based panels, such as plywood, laminated veneer lumber (LVL) and oriented strand board (OSB), etc. With the developing consideration of PF resin application, much more attention has been paid on its modification aimed to obtain desirable performance [2-4].

Many researchers have used a variety of methods to modify PF resins which has often resulted in improved performance characteristics [5-9]. Park et al modified a PF resin with three carbonates (i.e. propylene carbonate, sodium carbonate and potassium carbonate), where results

showed that all the carbonates can accelerate the cure rate of a PF resin and could reduce the pressing time for panel manufacture [5]. Gao et al indicated that a nanoscale copper oxide had the ability to reduce the activation energy of PF cure and improve the curing degree of a neat PF resin [6, 7]. PF resins have also been used as engineered wood composites applied to wood structure or timber architecture. Stark et al emphasized that PF resins are typically used in the construction of plywood and oriented strand board where exposure to weather is likely [8]. Gabrielli and Kamke reported the use of a PF resin combined with the viscoelastic thermal compression (VTC) process to produce a dimensionally stable and mechanically enhanced wood-based product [9].

In order to make wood-based panels better adapt to exterior applications where they could be confronted with severe climatic conditions, such as exposure to the sun and rain, insects, erosion, fungi, etc., some researchers have used wood preservatives to enhance outdoor bio resistance and durability [10-12]. Freeman and McIntyre have indicated that copper ions can demonstrate activity as algacides, bactericides, fungicides, insecticides and moldicides, and that copper-based preservatives have been widely and successfully used for more than a century because they are relatively easy to create as waterborne formulations and it is easy to analyze and determine the extent of their penetration in wood. For instance, the presence of copper in waterborne preservatives such as ACQ, copper citrate (CC), and CCA has been shown to stimulate production of 66 to 93 percent more oxalic acid compared to untreated controls within 2 weeks of exposure of blocks to test fungi [13, 14]. Gao and Du have shown that the use of nano cupric oxide to a PF resin can act against subterranean termites. Results from this study indicated that the weight loss of plywood decreased gradually from 31.12% to less than 10.37%, and the mortality of termites increased from 32.61% to higher than 86.35% [15]. Nano cupric oxide has been applied in many fields, such as in wood preservation, catalysis, and the development of antibacterial formulations,

due to its small size and high specific surface area [15, 16]. However, nano CuO powder is too expensive to modify PF resin directly [17, 18]. Thus, we considered combining nano CuO preparation and PF resin synthesis processing together because the price of copper salt is much lower than products of nano CuO powder. The preparation method of nano CuO includes liquid phase methods and solid phase methods [16]. Direct precipitation method belongs to liquid phase methods and this method is conducive to actual production. Also, the synthesis of direct precipitation is uncomplicated.

In this study, PF resin synthesis and nano copper oxide preparation were carried out in one system at the same time. Nano cupric oxide was prepared by a direct precipitation method. The significance of this work is to endow PF resin with the function of a wood preservative during preparation of the resin, and thus optimize the preservative treatment process of wood composites. This is also a cost-effective use of nano materials.

## 2. Experimental

### 2.1. Materials

Solid phenol,  $C_6H_6O$  (AR), formaldehyde solution, HCHO (AR, 37.0 wt/vol %), sodium hydroxide, NaOH, (AR), cupric sulfate,  $CuSO_4 \cdot 5H_2O$ , (AR) and polyvinyl alcohol (PVA) were obtained from Tianjin Fengchuan Chemical Reagent Technologies Co., Ltd, China. Polyvinyl pyrrolidone (PVP-K30) was purchased from Tianjin Guangfu Fine Chemical Research Institute, China. Different concentrations of polyvinyl alcohol solution, as shown in Table 1, were used as protective colloids and to increase the viscosity of modified adhesives. Polyvinyl pyrrolidone, a type of surfactant, was used in these experiments as a dispersant. Nano copper oxide was prepared by a precipitation method from copper sulfate and sodium hydroxide.

## 2.2. Synthesis of PF resin control

Phenol (155.55g), sodium hydroxide (49.65 g, 40.0 wt/vol %), and water (36.80 g) were placed in a 4-L reaction vessel with vigorous stirring at 40-50°C and for 10 minutes. The reaction vessel was equipped with a stirrer, a reflux condenser, a thermometer and a silicone flexible pipe. A substantial amount of the formaldehyde required for the preparation (193.2 g) was added to the reactor in five lots every 10 minutes. The reaction temperature was maintained at 40-50°C. After that, the reaction temperature was gradually raised to  $92 \pm 2^\circ\text{C}$  over a 50 minute period and maintained at this temperature for 15 minutes. Then the system was cooled to 80°C and a second portion of sodium hydroxide (16.55 g, 40.0 wt/vol %) and formaldehyde (48.3 g) were added in two steps over 30 minutes. The temperature was then increased to  $92 \pm 2^\circ\text{C}$  over a 10 minute interval and maintained at this temperature for 30 minutes. The system was then cooled to room temperature with cold water. The final product was obtained with a sodium hydroxide content of 5.30 wt% and pH value of  $11 \pm 0.5$ , with a molar ratio of formaldehyde to phenol of 1.8/1.0. The solid content and viscosity were 48.30 wt% and 132 mPa sec, respectively.

## 2.3. Preparation of nano CuO modified PF resins

Cupric sulfate solutions were prepared by dissolving  $\text{CuSO}_4 \cdot 5\text{H}_2\text{O}$  into water at 80°C. Nano CuO was synthesized by adding cupric sulfate solution to the basic alkaline PF resin. The amounts of  $\text{CuSO}_4 \cdot 5\text{H}_2\text{O}$ , PVP and PVA in the different samples prepared are shown in Table 1. The specific processes employed to prepare these resins are described below.

During the last step of the PF resin synthesis process before the resin was cooled to room temperature, the reaction temperature was reduced to 80 °C and then PVP was added. After the PVP had dissolved, PVA solution, prepared in advance, was placed into the reactor. Additional sodium hydroxide was then added to ensure the alkaline environment was maintained according to the reaction requirement of cupric sulfate. Then, a peristaltic pump was used to add cupric sulfate solution to the reactor regularly and quantitatively, with this conducted at 80°C for between 60 and 90 minutes duration. The experimental equipment employed in this process is shown in Fig. 1. The reaction was then continued for 50 minutes upon which the system was cooled to room temperature and the reaction products discharged from the reactor.

#### 2.4. Dynamic DSC analysis

A 204F1 calorimeter (Netzsch, Germany) was used to test the thermal behavior of the modified PF samples, which was equipped with a Proteus Analysis thermal analysis system. 5-10 mg specimens were placed in a hermetically sealed aluminum capsule. The samples were then heated from 40-450 °C in the presence of nitrogen gas (10mL/min) at heating rates of 5, 10, and 15 °C/min.

Using Equations (1) and (2), both the degree of conversion ( $\alpha$ ) and reaction rate ( $d\alpha/dt$ ) were calculated. Through the process of chain extension, chain branching, and cross linking, the conversion of PF resin can be defined as the transformation of small molecules to large molecules, which finally results in a three-dimensional network of infinite molecular weight [7, 19],

$$\alpha = \Delta H (t) / \Delta H_{RXN} \quad (1)$$

$$d\alpha/dt = dH / (dt\Delta H_{RXN}) \quad (2)$$

where  $\Delta H (t)$  is the partial heat of reaction at a specific curing time ( $t$ ),  $\Delta H_{RXN}$  is the total heat of

reaction, and  $dH/dt$  is the heat flow.

It is possible to evaluate the activation energy based on the above dynamic DSC results at a given degree of conversion  $E_\alpha$  according to the following procedures. The relationship between  $\alpha$  and  $k$  can be expressed as Equation (3),

$$d\alpha/dt = k(1 - \alpha)^n \quad (3)$$

$$k = A\exp(-E/RT) \quad (4)$$

where  $k$  is the reaction rate ( $s^{-1}$ ),  $n$  is the reaction order,  $A$  is the pre-exponential factor ( $s^{-1}$ ),  $E$  is the activation energy (J/mol),  $R$  is the universal gas constant (8.314 J/mol·K), and  $T$  is the absolute temperature (K).

The basic assumption of the isoconversional method is the reaction rate at constant extent of conversion is a function only of the temperature [20]. For model free analysis, the kinetics start with the basic rate equation that relates the rate of conversion at constant temperature,  $d\alpha/dt$ , to a function of the concentration of reactants,  $f(\alpha)$ , through the constant of reaction rate,  $k$ . If  $k$  is dependent on reaction temperature through the Arrhenius relationship, then a replaced equation (3) can be obtained as follows:

$$d\alpha/dT = (f(\alpha)/\Phi) A\exp(-E/RT) \quad (5)$$

where  $\Phi=dT/dt$  is the heating rate (K/min). In the isoconversional kinetic method, the parameters are independent of the heating rates, so corresponding parameters at different heating rates can be obtained [7]. The differential form of Equation (5) is expressed as Equation (6),

$$d \ln(d\alpha/dt)_\alpha/dT^{-1} = -E_\alpha/R \quad (6)$$

where  $E_\alpha$  is the activation energy at a given degree of conversion. Based on Equation (6), several methods have been suggested to calculate the  $E_\alpha$  value such as the Kissinger-Akahira-Sunose (KAS) algorithm and a method proposed by Vyazovkin [20, 21]. In this study, the KAS algorithm



was used to calculate  $E_\alpha$  as expressed in Equation (7),

$$\ln \Phi/T_i^2 = -E_\alpha/RT_i + \ln(RA/E_\alpha) \quad (7)$$

where  $T_i$  is the temperature to reach a given degree of conversion. A plot of  $\ln \Phi/T_i^2$  vs.  $1/T_i$  is a straight line from which the activation energy  $E_\alpha$  and pre-exponential factor  $A$  can be obtained from the slope and the intercept, respectively [7].

### 2.5. $^{13}\text{C}$ NMR test

NMR resin samples were prepared by mixing liquid resins of 200  $\mu\text{L}$  volume with 300 $\mu\text{L}$   $\text{D}_2\text{O}$ . Carbon spectra were obtained with a Bruker Avance III 600 MHz nuclear magnetic resonance spectrometer at a frequency of 150 MHz. The spectrum was recorded with a pulse angle of 90 degrees and the relaxation delay was 6s. Trimethylsilyl sodium propionate (TSP) was used to calibrate the zero position. To obtain the quantitative results, the inverse-gated decoupling method was applied by using the “zgig” pulse program.

### 2.6. Three layer plywood preparation and shear strength testing

The mechanical performance of the modified PF resin was tested by evaluating the shear strength of three layer plywood prepared in the laboratory. Three-layer plywood panels were prepared using Chinese white poplar (*populus tomentosa*) veneers of 400 (W)  $\times$  400 (L)  $\times$  3.5 (T)  $\text{mm}^3$ , which were obtained from a commercial plant in Hebei Province, China, and dried to approximately 3% moisture content before manufacturing. The glue spread used was 190  $\text{g}/\text{m}^2$  for both sides of middle panel. After a 10 minutes ageing stage, the mat was pressed for 4 minutes (50sec/mm), at 160 $^\circ\text{C}$  and 1.3 MPa. After hot pressing, the panels were cooled and conditioned at 22  $\pm$  1 $^\circ\text{C}$ , 65  $\pm$  2% relative humidity to a constant weight before testing. The shear strength with

seven repetitions was tested according to Chinese Standard GB/T 17657-1999 for plywood [22]. The shear strength was classified as six types according to the sample testing condition: 4 hours 100°C water boiling; 6 hours 100°C water boiling, dried 20 hours at  $63 \pm 3^\circ\text{C}$ , 6 hours 100°C water boiling; 24 hours room temperature water dipping; 4 days room temperature water dipping; 9 days room temperature water dipping; and 31 days room temperature water dipping respectively, all of which were followed by 10 minutes air-drying before testing.

An electromechanical universal testing machine (Model of UTM5105) was used to test the shear strength of plywood. The shear strength value of each sample was the mean of seven replicates per treatment. Significance of difference between means in each test condition was also analyzed by using a one-way ANOVA analysis at 95% confidence level with SPSS 22. Wood failure of each sample was estimated by visual measurement according to the damage within the shearing section and the adhesive layer.

### **3. Results and discussion**

#### *3.1. Effect of nanosize copper oxide on the dynamic DSC curves of PF resin*

Dynamic DSC is a common technique used to analyze the curing behavior of thermosetting resins. Figures 2 and 3 show the dynamic DSC curves of a PF resin control and PF modified by derived nano CuO. In general, all the samples showed the centralized exothermal range at around 300 to 340 °C. Furthermore, samples subjected to different heating rates were also reflecting a variety of changes. It is obvious that the peak temperature at a heating rate of 5 °C/min was lower than the heating rates of 10 °C/min and 15 °C/min in each group, which means that the curing temperature of the PF resin is related to the heating rate.

For a more detailed comparison between the PF control and the modified PF resins, all samples were subjected to a heating rate of 5 °C/min. The peak temperature of the PF control was 307.9 °C, while the corresponding temperatures for PCu-1 and PCu-4 were 321.6 °C and 329 °C respectively. The likely reason for this is that the introduction of derived nano CuO at concentrations of 1% and 12% has an influence on the condensation reaction. However, the peak temperatures for the PCu-2 and PCu-3 samples shifted to lower temperatures compared to the PF control, which means the combination with derived nano CuO with loading levels of 4% and 8% accelerated both the addition and condensation reactions and had a positive effect on the whole curing process. Much more detailed information on the curing process will be shown in the following results for activation energy and thermal enthalpy.

### 3.2. Curing kinetic analysis from dynamic DSC scanning

#### 3.2.1. Activation energy from ASTM E698-11

The curing kinetic analyses of exothermic reactions are significant in evaluating the properties of thermosetting resins. In this part, the activation energy ( $E_{698}$ ) can be defined as the apparent activation energy, which can be calculated at the exothermic peak of DSC cures. According to ASTM E698-11 [23], the specific formula is as follows.

$$E_{698} = -2.19R[d \log_{10}\beta/d (1/T)](8)$$

where  $R$  = gas constant (=8.314 J mol<sup>-1</sup> K<sup>-1</sup>),  $\beta$  is the heating rate (K/min), and  $T$  is the corrected peak maximum temperature in Kelvin. A plot of  $\log_{10}\beta$  versus  $1/T$ , allows the construction of a least squares “best fit” line. The slope of this line is taken as the value for  $d \log_{10}\beta/d (1/T)$ . The apparent activation energy of all samples are listed in Table 2.

The  $E_{698}$  value of the PF control was 104.23 KJ/mol, while the corresponding value of PCu-1 was 194.51 KJ/mol. This result is similar to a previous report, which indicated that the addition of nano CuO alone increased the apparent energy of the PF marginally from 31.71 to 33.40 KJ/mol [7]. The difference between these two values may be due to different synthetic methods for the preparation of nano CuO (synthesized by a precipitation method in this study versus the direct addition of nano CuO powder to a PF resin as described in a previous report [7]). Furthermore, a loading of nano CuO at 12% made the  $E_{698}$  increase significantly to 405.47 KJ/mol, with one possible reason being that the introduction of large amount of derived nano CuO hindered the whole curing process.

However, the  $E_{698}$  value of PCu-2 and PCu-3 declined to 95.74 and 101.47 KJ/mol respectively. The proportion of derived nano CuO and surfactant may be the reason for this change. While all four volumes of surfactant addition can be used to disperse nano CuO in an aqueous PF resin, it is obvious that PCu-2 showed the most positive effect.

### 3.2.2. Reaction enthalpy

Figure 4 shows the changes on the reaction enthalpy of different PF resins, which was tested by evaluating the differences using a one-way ANOVA analysis at 95% confidence level with SPSS 22. Since the curing reaction is complicated and exothermic, it can be assumed that analyzing reaction enthalpy is helpful in assessing the completion of the curing reactions. The enthalpy value of the PF control was 682 J/g, whereas it was reduced by introducing derived nano CuO at loading levels of 1, 8, and 12%. That means the exothermic enthalpy of corresponding samples are less than the PF control and it is not conducive to complete curing of the PF resin.

Specifically, the PCu-4 sample exhibited a reaction enthalpy decline from 682 to 446 J/g, which means much more reaction energy was needed for the PF resin to conduct both addition and condensation reactions with the derived nano CuO loading level at 12%.

However, the PCu-2 sample exhibited an enthalpy value which had increased to 788 J/g. This means the curing reaction of PF resin was accomplished much more completely with a derived nano CuO at a 4% load level imparting an improvement in the whole reaction process. Although the reaction enthalpy values are quite different, the samples between the PF control and PCu1-3 are not significantly different as indicated from the significance analyses.

### 3.2.3. *Activation energy from model free kinetic technique*

It is difficult to use a single apparent activation energy value to express the detailed reactions which occur during cure of a PF resin. The curing process of a PF resin is very complicated, which is characterized by the various functional groups of the phenol oligomer which are variably reactive, with addition and condensation reactions occurring simultaneously [24]. This means that the degree of conversion of the overall reaction process plays an important role in analyzing the activation energy of reaction [25, 26]. The presence of nano CuO makes the curing process of a PF resin even more complicated, because of the molecular structure change of the PF resin and the complicated reactions amongst nano CuO, PVA, surfactant and PF resin.

In order to determine more details about the modification effect on PF resin curing, the dependence of activation energy on the degree of conversion was investigated using the model-free kinetic technique and the results are shown in Fig. 5. For PF control, the activation

energy started at around 216.2 KJ/mol and then increased marginally to 253.5 KJ/mol with the conversion percent of 5%. While the conversion degree was less than 60%, the activation energy of the PF control was maintained at approximately 250 KJ/mol. After that, the value of activation energy climbed slowly to the maximum value of 432.3 KJ/mol at the conversion degree of 95%. As the PF resin control completed the curing process, its activation energy went back to 266.0 KJ/mol. The tendency described above is consistent with the previous report [7]. While the PF resin control was modified by derived nano CuO, the relation of conversion degree to activation energy was varied. With the exception of PCu-1, the original activation energy of the modified samples was higher than the PF control, which is related to the phase change of PF resin caused by the addition of nano sized CuO. Furthermore, the increases in original activation energy means that the condensation reaction of the PF resin became more difficult with the introduction of the derived nano CuO.

The interesting result is that the trend of activation energy of PCu-2 and PCu-3 at the initial stage is completely different with that of the PF control. As the activation energy of the PF control started to climb before a degree of conversion of 5%, the related value of PCu-2 dropped substantially before a degree of conversion of 20%. The same trend can be observed with PCu-3, but its activation energy ceased decreasing at a degree of conversion of 10%. The opposite trend with PCu-2 and PCu-3 is probably related to the effect of derived nano CuO at the corresponding load level. Thus, derived nano CuO introduced at a loading level of 4 to 8% is positive in contributing to the initiation of the condensation reaction of PF resin. As the degree of conversion reached 20%, the activation energy of samples PCu-1 and PCu-4 was much higher than the PF control. However, the phenomena was changed as the degree of conversion reached 75%, which means that much more energy was needed for the PF resin to continue with the condensation

reactions with nano CuO loading levels of 1% and 12%. However, within the same degree of conversion range, the tendency and the exact value of activation energy from PCu-2 and PCu-3 was similar to the PF control.

Towards the later stage of the curing process (exactly after 80% degree of conversion), the relationship between activation energy and degree of conversion is varied as PF resin modified by derived nano CuO. However, the ending activation energy value of all samples reached together at around 266.0 KJ/mol. So, the curing characteristics of the derived nano CuO modified PF resin is dependent on the loading level of nano CuO. The mentioned analysis is consistent with the result of reaction enthalpy shown in Fig. 4, where the enthalpy values of PCu-1 and PCu-4 are lower than with the PF control. The apparent activation energy of  $E_{698}$  listed in Table 2 also proved that the condensation reactions for samples PCu-1 and PCu-4 became difficult compared to the PF control.

### 3.3. $^{13}\text{C}$ NMR spectrum analysis

#### 3.3.1. Peak assignment of PF resin control

The spectrum of pure PF resin is shown in Fig. 6a, and some representative function group assignments are listed in Table 3. The peak at 158.59 ppm was attributed to phenoxy carbons. Substituted *para* carbons was considered at 132.64 ppm, unsubstituted *meta* carbons and substituted *ortho* carbons was near them at around 130.61 ppm. The peak position of unsubstituted *para* and *ortho* carbons were at 119 ppm approximately, and the corresponding peak area was much less than substituted aromatic carbons, which means most of the aromatic carbons are involved in condensation reactions. In the high field region, the derived PF resin peaks are separated significantly than those in the low field. The chemical shifts at 66.73 ppm and 63.85 ppm were assigned to the dimethylene ether bridges and carbons of methylol groups in the benzene ring

respectively. The peak of methanol carbons was more explicit at 51.73 ppm. At the positions of 42.3 ppm and 37.29 ppm, there were *para-para* methylene bridges and *para-ortho* methylene bridges respectively.

### 3.3.2. Effect of nano CuO on the molecular structure change of PF resin

Cross-polarization and magic angle spinning  $^{13}\text{C}$  NMR (CP/MAS) spectra of liquid PF resins modified by derived nanometer CuO with different loading levels are shown in Fig. 6b to e. The chemical shift changes of each functional group are summarized in Table 3. For the PF samples which were synthesized under alkaline conditions, the spectra became more chaotic and were characterized with a lower signal-to-noise ratio at the baseline as the nano CuO loading level increased. For instance, extra sodium hydroxide was added to PCu-1 to 4 compared with the PF control. In contrast to the reference values [27, 28], the peak positions of all samples were generally offset to the low field, such as unsubstituted *para* and *ortho* carbons, methanol, and methylene bridges. The probable reason is that the solvent effect leads to this phenomenon [28]. More specifically, in the process of synthesizing derived nanometer CuO, excess water was introduced to dissolve  $\text{CuSO}_4 \cdot 5\text{H}_2\text{O}$ .

Several peaks at around 166 ppm could be attributed to carbonyl [29]. According to the basic principles of nuclear magnetic resonance and organic chemistry, it can be deduced that this position is sodium formate. More specifically, in the alkaline environment, a complex disproportionation reaction of formaldehyde would occur and generate formic acid and methanol, resulting in sodium ions reacting with formic acid to produce sodium formate. The chemical shift of functional groups would be affected by the introduction of nanosize copper oxide, which can be



observed from the chemical shift of phenoxy carbons which were gradually shifted to the lower field as copper ions. The chemical shift moved to lower field from 158.59 ppm to 162.66 ppm as the derived nano CuO level was increased to 12%. The probable reason for this is that the copper ions would have reacted with oxygen on the phenolic hydroxyl groups via a complexation reaction. The electronic cloud density of the phenoxy carbons decreased resulting in the chemical shift moving to a lower field region. The chemical shifts of hydroxymethyl carbons on the benzene ring also showed the same tendency. But the trend is less significant than that from phenoxy carbons. We suspect that, in the strong basic condition, phenol resonance could produce phenol anions which would off the domain, thus the complexation reaction would be easier to carry out. In contrast, the hydrogen ion in the hydroxymethyl on the benzene ring would affect the progress of this reaction.

### 3.3.3. Quantitative analysis of PF resin control and modified PF resin

In order to analyze the changes of chemical groups more intuitively, quantitative structural analysis was used and all integration values are listed in Table 4. The peak area from the methanol carbon was set at 1 statistically, and then the corresponding areas of other peaks were calculated. From the integration values demonstrated in Table 4, it can be seen that derived nano CuO has a significant effect on functional group changes. Overall, the amount of substituted *para* carbons on phenol rings was much higher than substituted *ortho* carbons for each tested group. The probable reason is that the reactivity of the *para* hydrogens on the phenol rings is higher than that observed from the *ortho* positions. Furthermore, specific changes of substituted carbons in phenol rings are described in below. The integrated values of substituted *para* carbons were observed to increase with increasing derived nano CuO loading level. However, the *meta* carbons and substituted *ortho*

carbons showed an opposite trend, and the integrated values were found to decrease from 0.76 to 0.17 as the loading level of derived nano CuO reached 12%.

The results indicated that the introduction of nano CuO had a positive effect on *para* substituted reactions, and delayed *meta* and *ortho* substituted reactions simultaneously. Thus, connections contributed from *para* carbons increased in the modified PF resin system. In addition, the calculated values of substituted *ortho* carbons reduced, while the unsubstituted *ortho* carbons changed slightly with the exception of PCu-3. The probable reason for this result is that nano CuO improved the addition reactions of *para* carbons on phenol rings.

The synthesis of PF resin includes both addition and condensation reactions. The reaction of phenol with formaldehyde generates methylol phenols. Thus, the integration values of methylol groups can be used to characterize the extent to which addition reactions occur, while the amount of methylene bridges has the same effect for describing the extent of condensation reactions. Calculated values of methylol groups were higher than methylene bridges as listed in Table 4, which means the rate of addition reactions is much higher than that of condensation reactions.

The methylol groups values for the modified PF resins were higher than that observed in the PF resin control, which indicates that the derived nano CuO enhanced the existence of addition reactions during the cure process. Under alkaline conditions, in which condensation reactions would be favoured, cured polymer would be mainly linked by methylene bridges. The sum of *para/para* methylene bridges and *para/ortho* methylene bridges in modified PF resins were raised in comparison to that of the PF resin control, which indicates that the introduction of nano CuO favours the existence of condensation reactions.

### 3.4. Shear strength of three layer plywood

The shear strength values of three layer plywood specimens are listed in Table 5. The variation of shear strength under different test conditions is not remarkable, and what is interesting is that the modification process did not significantly influence the bonding performance of plywood. Following insertion in boiling water for 4 hours, there was little difference between the modified samples and the control group. But after 6 hours, the shear strength of the modified groups decreased slightly. As industry has paid much more attention to plywood application under more moderate conditions, the room temperature water resistance and mechanical properties were also evaluated. The results obtained indicated that the shear strength of modified samples decreased slightly after soaking for several days, which means that the water resistance of the glue line in modified samples declined slightly in comparison to the PF resin control.

According to Chinese Standards GB/T 17657-1999 [22] and GB/T 9846.3-2004 [30], the test conditions for class I plywood are 4 hours 100°C water boiling, followed by drying for 20 hours at  $63 \pm 3^\circ\text{C}$ , followed by a further 4 hours 100°C water boiling, with the standard value of bonding strength for class I plywood being at least 0.7MPa. Thus, the second column of results shown in Table 5 has met the requirements of the above Chinese Standards. Considering that the wood composite is more likely to be affected by ambient water, we have added several other test conditions with all results meeting the requirements of these Chinese Standards. Furthermore, wood failure was reduced with loading levels of nano CuO at 8% and 12%. PVP, with hydrophilic properties, was used here as dispersant in the system. The probable reason for the decrease of wood failure can be attributed to the amount of PVP increasing simultaneously with loading level of CuO, which is sensitive to absorbed water, and then influences the cross linking in the plywood

glueline. However, the shear strength results of all samples met the requirements of the previously mentioned Chinese Standards [22, 30]. Further research will focus on modifying the synthesis process and hot pressing parameters to improve the water resistance of bonded wood composites.

Our goal in this study was to combine nanosize cupric oxide with PF resin to bond wood based composites, and then to introduce bio-resistance to such composites for potential use in products such as oriented strand board (OSB), laminated veneer lumber (LVL), and wafer board, etc. Although in some cases the shear strength of composites were shown to decline following the incorporation of CuO, the overall performance indicated that derived nano CuO has the potential to perform as a wood preservative.

#### 4. Conclusions

In this study, the direct precipitation method was used to synthesize nanometer-sized cupric oxide with results showing that the synthesis process was feasible. When incorporated into a PF resin the introduction of different concentrations of nano CuO had a positive effect on the curing process. Loading levels of 4% and 8% reduced the values of apparent activation energy slightly, indicating that the combination of derived nano CuO at this loading level can accelerate both the addition and condensation reaction rates. The changes of reaction enthalpy showed that the sample of PCu-2 exhibited increased value, while the corresponding value of PCu-3 decreased slightly but not significant in statistically. The relation between activation energy and degree of conversion confirmed the above result with the formulations PCu-2 and PCu-3 demonstrating a positive effect on the curing process.

With the introduction of derived nano CuO, the chemical shifts of all samples were generally

offset to the low field for the solvent effect. Complexation reactions between copper ions and oxygen on the phenolic hydroxyl groups had an influence on the phenoxy carbons. According to quantitative analysis, nano CuO had a positive effect on the *para* substituted reaction which could enhance the efficacy of both the addition and condensation reactions, which is consistent with DSC results. Furthermore, the shear strength of the modified samples declined slightly compared with PF control in each test condition, but they all met the requirements of the Chinese Standards, thus indicating potential for application in engineering wood composite preservation.

Future work will focus on the effect of particulate size of derived nano CuO on the bio resistance of engineered wood composites bonded by the modified PF resin adhesive.

### **Acknowledgement**

The authors express their gratitude to the National Natural Science Foundation of China (granted 31660175), for their financial support to this research work, and also thanks to the support from the Project of Yunnan Reserve Talents of Young Academic and Technical Leaders.

### **References**

- [1] Pizzi A, Mittal KL. Handbook of Adhesive Technology. 2nd ed. Revised and Expanded, CRC Press; 2003.
- [2] Wang J, Jiang H, Jiang N. Study on the pyrolysis of phenol-formaldehyde (PF) resin and

modified PF resin. *Thermochim Acta* 2009; 496: 136-42.

[3] Park B-D, Riedl B, Hsu EW, Shields J. Application of cure-accelerated phenol-formaldehyde (PF) adhesives for three-layer medium density fiberboard (MDF) manufacture. *Wood Sci Technol* 2001; 35: 311-23.

[4] Abdalla MO, Ludwick A, Mitchell T. Boron-modified phenolic resins for high performance applications. *Polymer* 2003; 44: 7353-59.

[5] Park B-D, Riedl B, Hsu EW, Shields J. Differential scanning calorimetry of phenol-formaldehyde resins cure-accelerated by carbonates. *Polymer* 1999; 40: 1689-99.

[6] Gao W, Cao J, Kamdem DP. Effect and mechanism of nanosize copper oxide on some physical and mechanical properties of flakeboards. *Maderas-Cienc Tecnol* 2011; 13: 203-10.

[7] Gao W, Du G. Curing kinetics of nano cupric oxide (CuO)-modified PF resin as wood adhesive: effect of surfactant. *J Adhes Sci Technol* 2013; 27: 2421-32.

[8] Stark NM, Cai Z, Carll C. Wood-based composite materials: panel products, glued-laminated timber, structural composite lumber, and wood-nonwood composite materials. *Wood handbook: Wood as an engineering material*. Centennial ed. Createspace; 2010.

[9] Gabrielli CP, Kamke FA. Phenol-formaldehyde impregnation of densified wood for improved dimensional stability. *Wood Sci Technol* 2010; 44: 95-104.

[10] Muin M, Tsunoda K. Preservative treatment of wood-based composites with 3-iodo-2-propynyl butylcarbamate using supercritical carbon dioxide impregnation. *J Wood Sci* 2003; 49: 430-6.

[11] Tascioglu C, Goodell B, Lopez-Anido R. Bond durability characterization of preservative treated wood and E-glass/phenolic composite interfaces. *Compos Sci Technol* 2003; 63: 979-91.

[12] Smith WR, Wu Q. Durability improvement for structural wood composites through chemical

treatments. *Forest Prod J* 2005; 55: 8-17.

[13] Freeman MH, McIntyre CR. A comprehensive review of copper-based wood preservatives with a focus on new micronized or dispersed copper systems. *Forest Prod J* 2008; 58: 6-27.

[14] Green III F, Clausen CA. Copper tolerance of brown-rot fungi: time course of oxalic acid production. *Int Biodeter Biodegr* 2003; 51: 145-9.

[15] Gao W, Du G. Physico-mechanical properties of plywood bonded by nano cupric oxide (CuO) modified PF resins against subterranean termites. *Maderas-Cienc Tecnol* 2015; 17: 129-38.

[16] Lei T, Li F, Wang Y, Wang Y, Yang S. Preparation and application of nano copper oxide powder. *Chem Ind Eng Prog* 2013; 32: 2429-33.

[17] Sigma-Aldrich. China-Mainland, <http://www.sigmaaldrich.com/catalog/product/Aldrich/544868?lang=zh&region=CN>.

[18] Sigma-Aldrich. China-Mainland, <http://www.sigmaaldrich.com/catalog/product/sigald/c7631?lang=zh&region=CN>.

[19] Wang XM, Riedl B, Christiansen AW, Geimer RL. The effects of temperature and humidity on phenol-formaldehyde resin bonding. *Wood Sci Technol* 1995; 29: 253-66.

[20] Vyazovkin S, Sbirrazzuoli N. Kinetic methods to study isothermal and nonisothermal epoxyanhydride cure. *Macromol Chem Phys* 1999; 200: 2294-303.

[21] Vyazovkin S, Sbirrazzuoli N. Isoconversional kinetic analysis of thermally stimulated processes in polymers. *Macromol Rapid Comm* 2006; 27: 1515-32.

[22] Chinese Standard. GB/T 17657-1999; 1999.

[23] ASTM E698-11. In Standard Test Method for Arrhenius Kinetic Constants for Thermally Unstable Materials Using Differential Scanning Calorimetry and the Flynn/Wall/Ozawa Method. West Conshohocken; 2011.

- [24] Gardziella A, Pilato LA, Knop A. Phenolic Resins: Chemistry, Application, Standardization, Safety and Ecology. 2nd ed. Springer, Berlin Heidelberg; 2000.
- [25] Li S, Vuorimaa E, Lemmetyinen H. Application of isothermal and model-free isoconversional modes in DSC measurement for the curing process of the PU system. *J Appl Polym Sci* 2001; 81: 1474-80.
- [26] Riedl B, He G. Curing kinetics of phenol formaldehyde resin and wood-resin interactions in the presence of wood substrates. *Wood Sci Technol* 2004; 38: 69-81.
- [27] Rego R, Adriaensens PJ, Carleer RA, Gelan JM. Fully quantitative carbon-13 NMR characterization of resol phenol-formaldehyde prepolymer resins. *Polymer* 2004; 45: 33-8.
- [28] Holopainen T, Alvila L, Rainio J, Pakkanen TT. Phenol-formaldehyde resol resins studied by  $^{13}\text{C}$ -NMR spectroscopy, gel permeation chromatography, and differential scanning calorimetry. *J Appl Polym Sci* 1997; 66: 1183-93.
- [29] He G, Yan N.  $^{13}\text{C}$  NMR study on structure, composition and curing behavior of phenol-urea-formaldehyde resole resins. *Polymer* 2004; 45: 6813-22.
- [30] Chinese Standard. GB/T 9846.3-2004; 2004.

FIG. 1. Nano CuO modified PF resin synthesis process and generation equipment.

FIG. 2. Dynamic DSC curves of PF resin control and PF modified by nano CuO at a heating rate of  $5\text{ }^{\circ}\text{C}/\text{min}$ .

FIG. 3. Dynamic DSC curves of PF control (a) and PCu-1 at CuO loading level of 1% (b), PCu-2 at CuO loading level of 4% (c), PCu-3 at CuO loading level of 8% (d), and PCu-4 at CuO loading

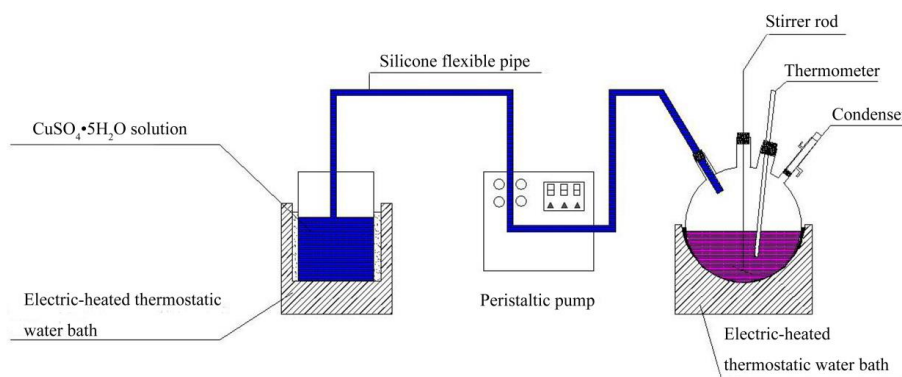


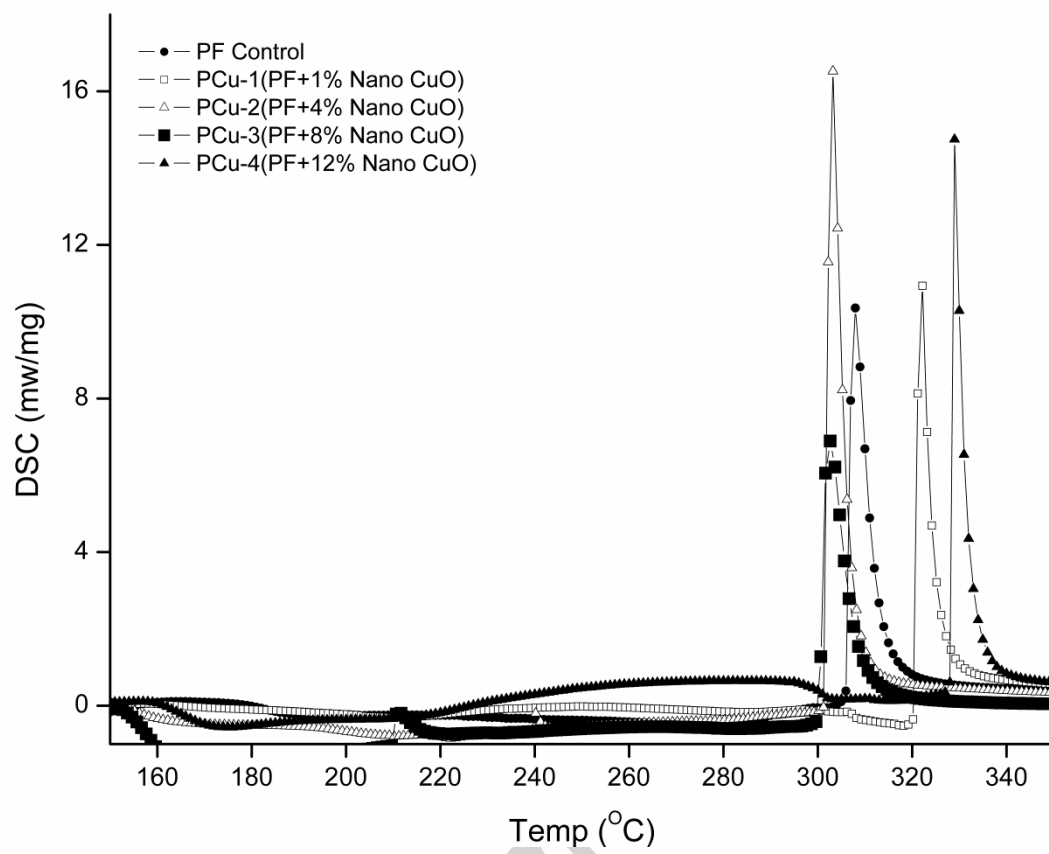
level of 12% (e) at heating rate of 5, 10, and 15°C/min respectively.

FIG. 4. Enthalpy of PF resin control and PF resin modified by nano CuO. A column labeled by the same letter is not significantly different using Tukey's studentized range test ( $\alpha = 0.05$ ).

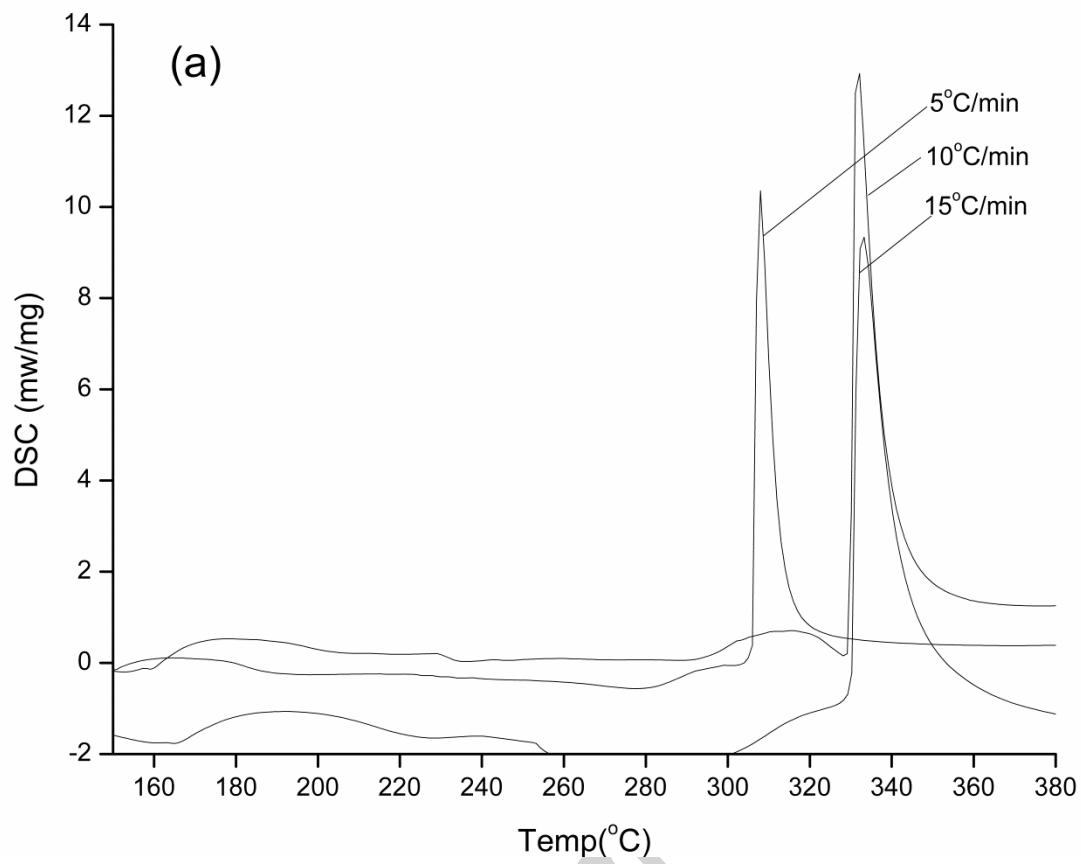
FIG. 5. The dependence of activation energy on the degree of conversion for PF resin control and PF resin modified by nano CuO from model-free kinetic technique.

FIG. 6. The  $^{13}\text{C}$  NMR spectrum of PF control (a) and PCu-1 at CuO loading level of 1% (b), PCu-2 at CuO loading level of 4% (c), PCu-3 at CuO loading level of 8% (d), and PCu-4 at CuO loading level of 12% (e) respectively.

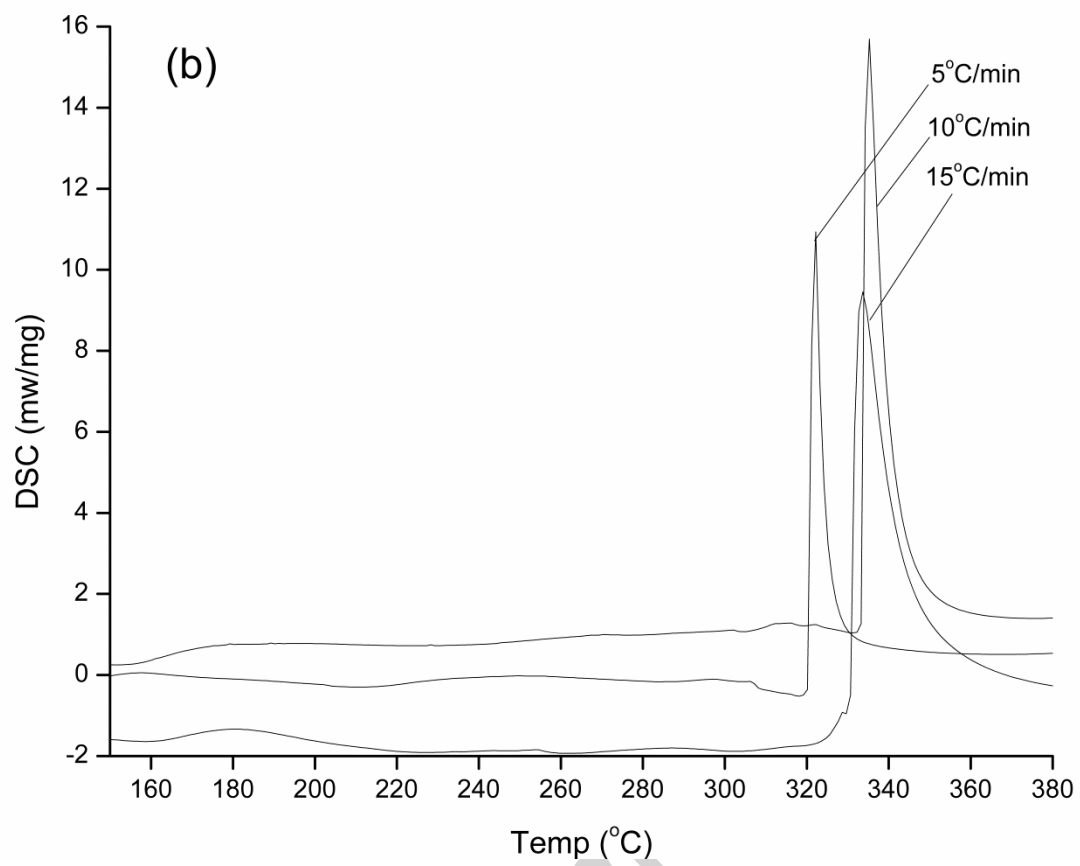


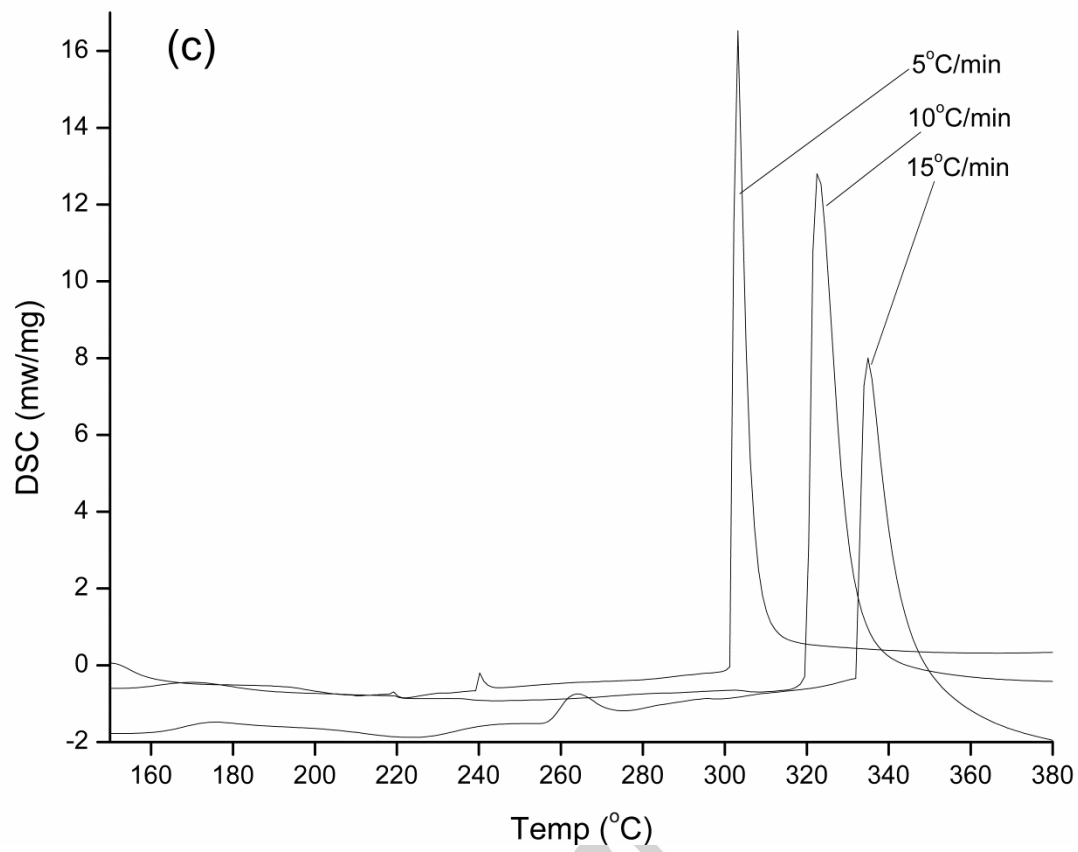


Accepted manuscript

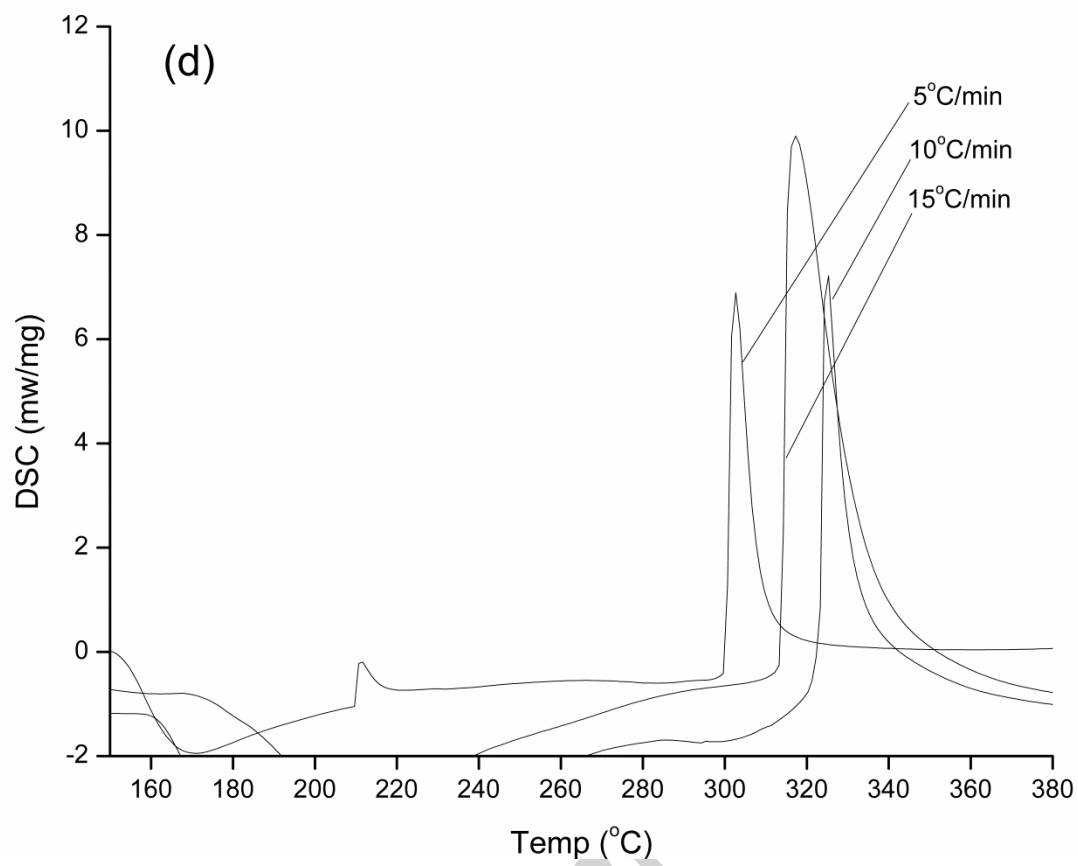


Accepted m.

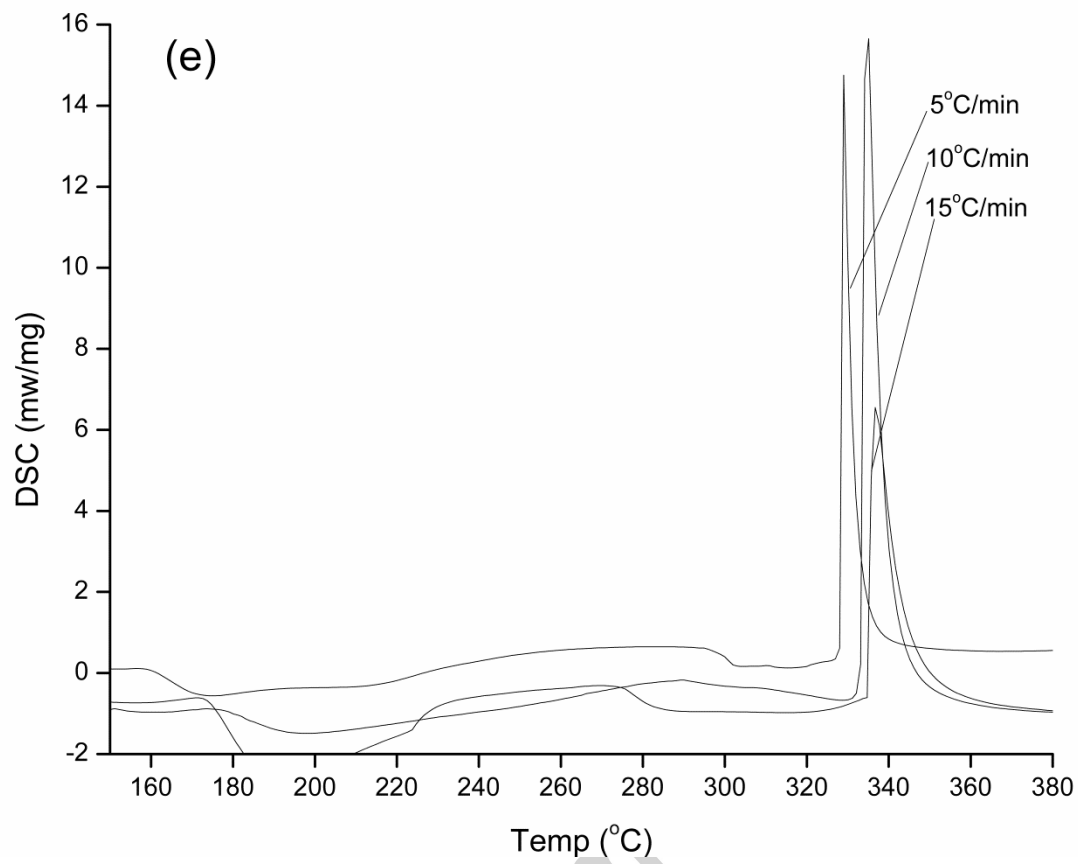




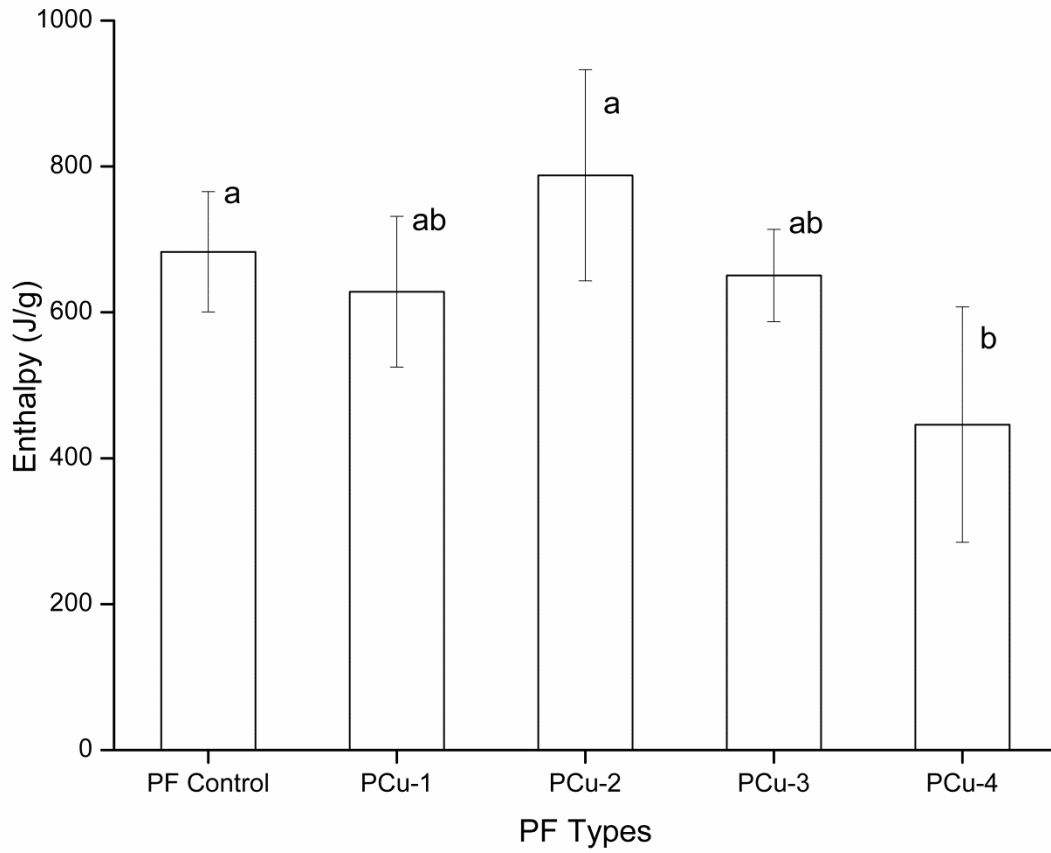
Accepted m



Accepted m

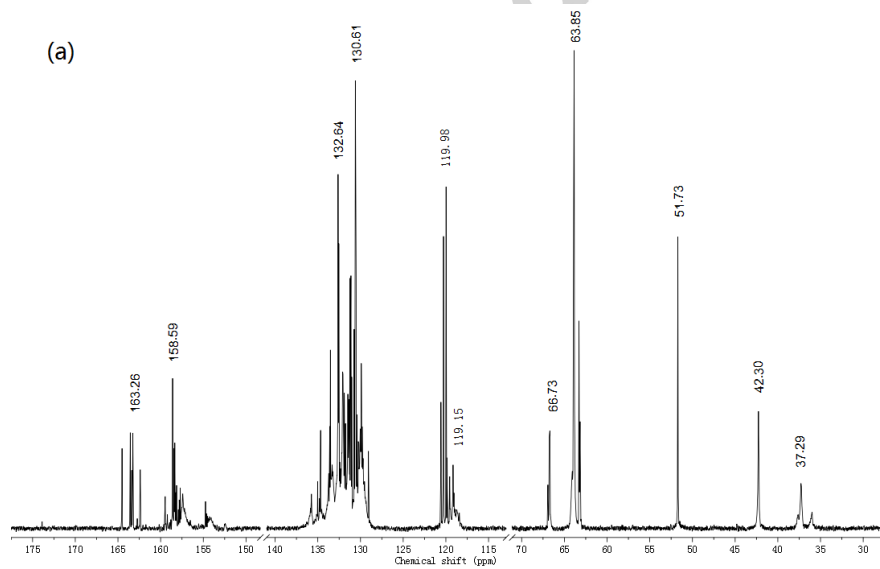
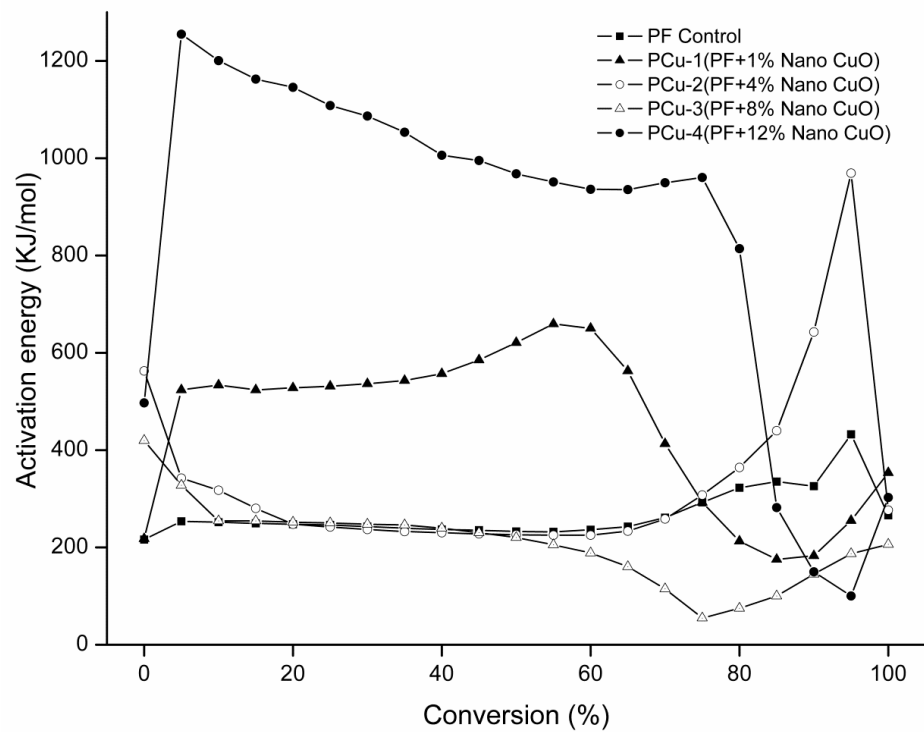


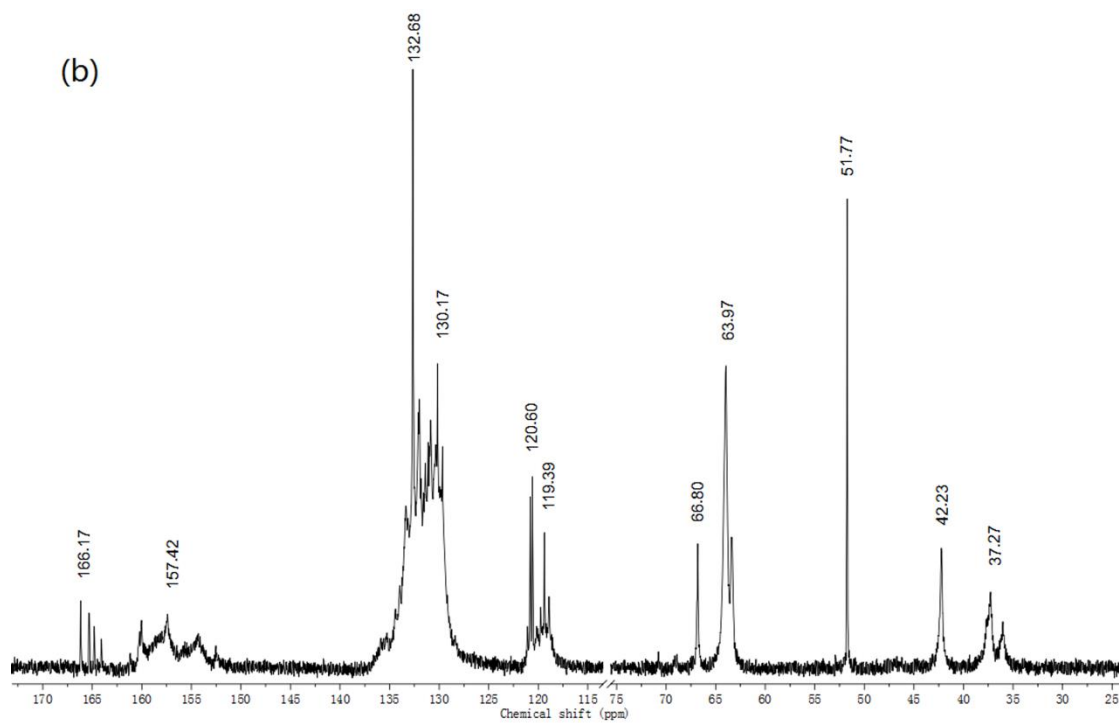
Accepted m



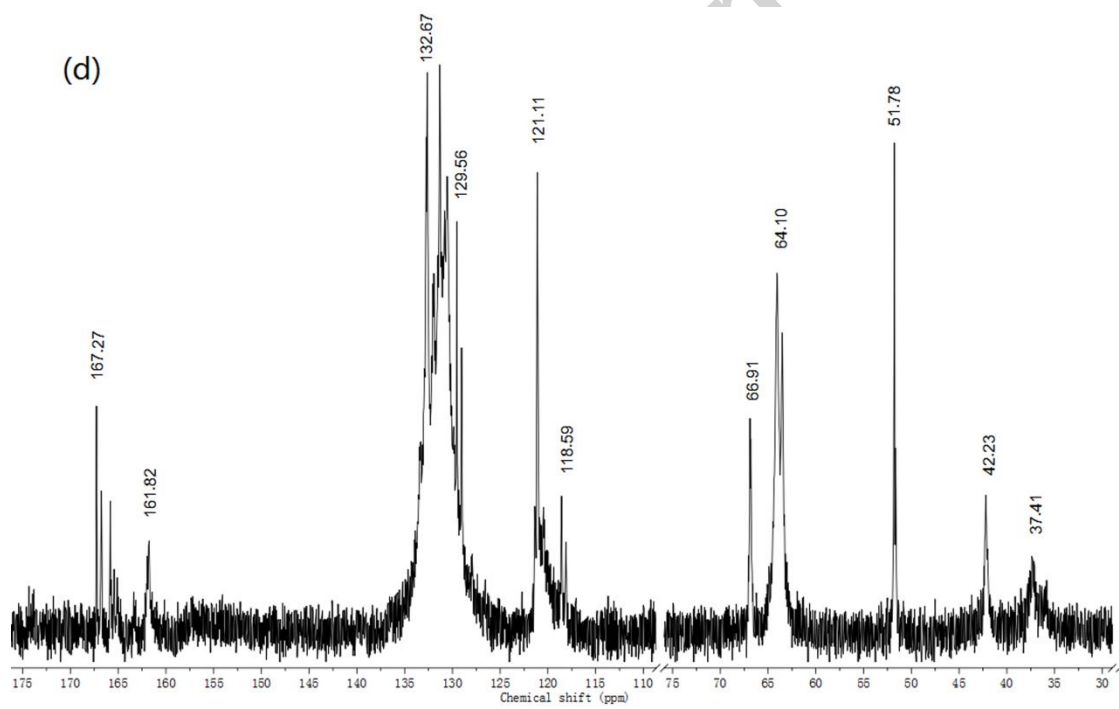
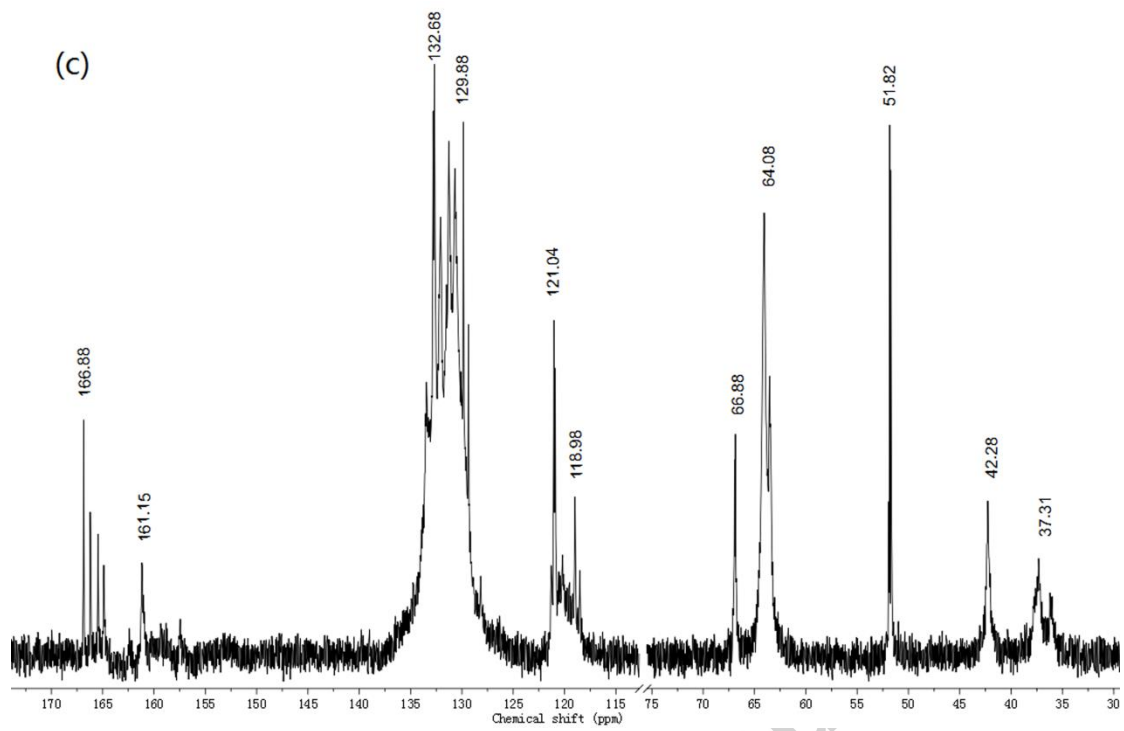
Accepted m

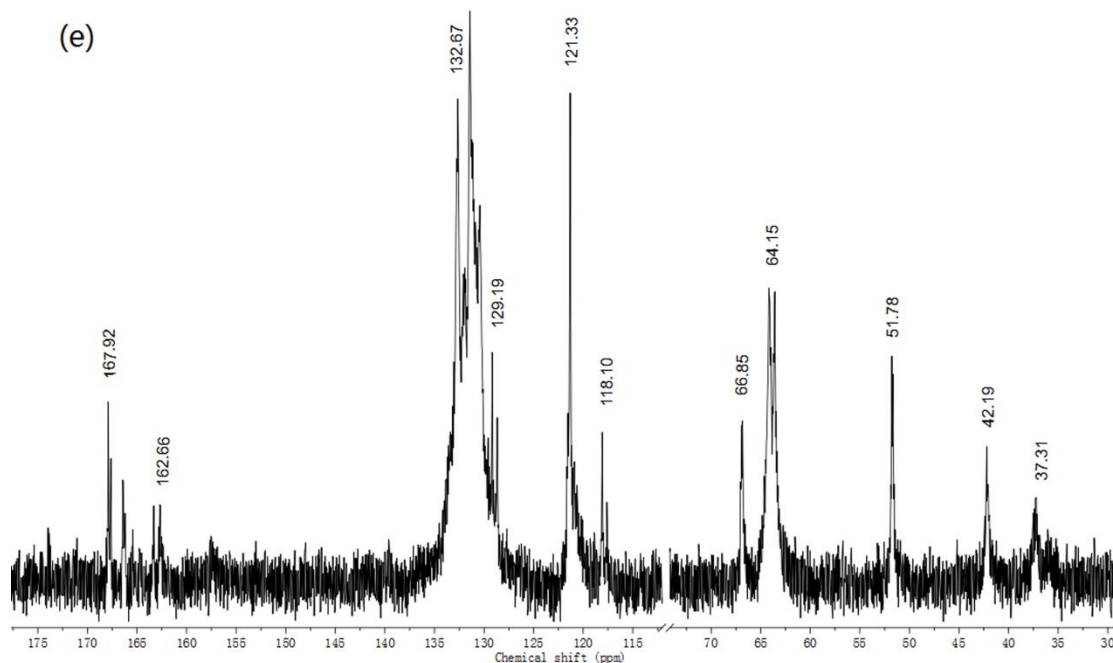






Accepted manu





**Table 1** The additive amount of  $\text{CuSO}_4 \cdot 5\text{H}_2\text{O}$ , PVP, PVA and the concentration of PVA.

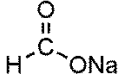
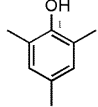
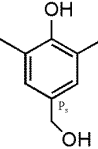
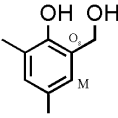
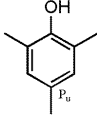
Sample	CuO (%)	CuO (g)	$\text{CuSO}_4 \cdot 5\text{H}_2\text{O}$ (g)	PVP (g)	PVA (g)	Concentration of PVA (%)
PF Control	0	0	0	0	0	0
PCu-1	1	5	15.6	0.05	50	5
PCu-2	4	20	62.5	0.26	70	5
PCu-3	8	40	125.0	0.68	68.75	8
PCu-4	12	60	187.5	1.20	93.75	8

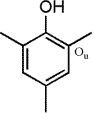
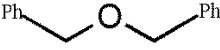

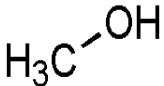
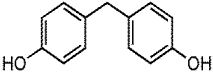
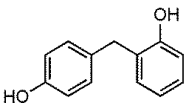
\* The total weight of PF control is 500g. The addition of nano CuO from samples PCu-1, 2, 3, 4 are based on the weight 1%, 4%, 8%, and 12% of PF control. The addition of PVA from samples PCu-1, 2, 3, 4 are based on the weight 0.5%, 0.7%, 1.1%, and 1.5% of PF control. The addition of PVP from samples PCu-1, 2, 3, 4 are based on the weight 1%, 1.3%, 1.7%, and 2% of nano CuO.

**Table 2** DSC parameters of PF resin control and PF resin modified by nano CuO.

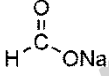
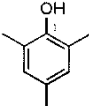
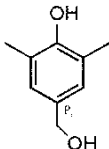
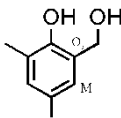
Sample	$E_{698}$ (KJ/mol)	$T_p$ (°C)		
		5 (°C/min)	10 (°C/min)	15 (°C/min)
PF control	104.23	307.9	331.7	333
PCu-1	194.51	321.6	335	333.6
PCu-2	95.74	302.9	322.8	334.9
PCu-3	101.47	302.5	324.8	317.2
PCu-4	405.47	329	334.7	336.9

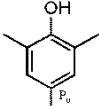
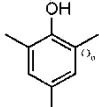
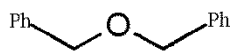

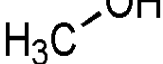
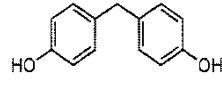
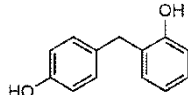
**Table 3**  $^{13}\text{C}$  NMR chemical shifts and group assignment of PF resin control and PF resin modified by nano CuO.

Function Group	Assignment	Chemical shift (ppm)					Reference
		PF control	PCu-1	PCu-2	PCu-3	PCu-4	
	Sodium formate	163.26	166.17	166.88	167.27	167.92	158-163 [22]
	Phenoxy carbons	158.59	157.42	161.15	161.82	162.66	148-160 [20]
	Substituted <i>para</i> carbons ( $P_s$ )	132.64	132.68	132.68	132.67	132.67	132-137 [20]
	<i>meta</i> Carbons (M) and substituted <i>ortho</i> carbons ( $O_s$ )	130.61	130.17	129.88	129.56	129.19	123-132 [20]
	Unsubstituted <i>para</i> carbons ( $P_u$ )	119.98	120.60	121.04	121.11	121.33	118-122 [20]

	Unsubstituted <i>ortho</i> carbons (O <sub>u</sub> )	119.15	119.39	118.98	118.59	118.10	111-118 [20]
	Dimethylene ether bridges (DMEB)	66.73	66.80	66.88	66.91	66.85	65-75 [20]
	Methylol groups (MG)	63.85	63.97	64.08	64.10	64.15	58-63 [20]
	Methanol	51.73	51.77	51.82	51.78	51.78	49.80 [21]
	<i>para/para</i> Methylene bridges (MBp/p)	42.3	42.23	42.28	42.23	42.19	39-42 [20]
	<i>para/ortho</i> Methylene bridges (MBp/o)	37.29	37.27	37.31	37.41	37.31	34-36 [20]

**Table 4** Quantitative analysis of chemical groups of PF resin control and modified PF resin via derived nano CuO.

Function Group	Assignment	Calculation				
		PF control	PCu-1	PCu-2	PCu-3	PCu-4
	Sodium formate	0.31	0.16	0.23	0.43	0.29
	Phenoxy carbons	0.38	0.36	0.41	0.26	0.23
	Substituted <i>para</i> carbons (P <sub>s</sub> )	1.82	1.04	1.22	2.60	2.23
	<i>meta</i> Carbons (M) and substituted <i>ortho</i> carbons (O <sub>s</sub> )	0.76	0.52	0.24	0.41	0.17

	Unsubstituted <i>para</i> carbons (P <sub>u</sub> )	0.61	0.35	0.32	0.35	0.31
	Unsubstituted <i>ortho</i> carbons (O <sub>u</sub> )	0.33	0.20	0.25	0.48	0.27
	Dimethylene ether bridges (DMEB)	0.68	0.43	0.74	1.27	0.82
	Methylol groups (MG)	4.21	5.36	5.31	8.64	4.31
	Methanol	1.00	1.00	1.00	1.00	1.00
	<i>para/para</i> Methylene bridges (MBp/p)	1.15	1.47	1.27	1.77	0.85
	<i>para/ortho</i> Methylene bridges (MBp/o)	0.76	1.66	1.37	1.02	0.43

\*For each tested sample, the peak area from Methanol carbon was set as 1 in statistically. Then other peaks corresponding area value will be calculated in relatively as listed in above table.

**Table 5** Shear strength of three veneers plywood bonded by PF control and all modified PF resins at six testing conditions.

Sample	Shear Strength (MPa)					
	4 hours 100°C water	6 hours 100°C water/dried 20 hours at 63°C/6 hours 100°C water	24 hours room temperature water	4 days room temperature water	9 days room temperature water	31 days room temperature water
PF Control	1.14 (0.17) a <u>96</u>	1.21 (0.15) a <u>100</u>	1.37 (0.14) a <u>96</u>	1.41 (0.08) a <u>100</u>	1.21 (0.10) ab <u>100</u>	1.21 (0.22) a <u>100</u>
PCu-1	1.18 (0.04)	0.98 (0.05) b <u>100</u>	1.13 (0.13) b <u>100</u>	1.08 (0.13) bd <u>98</u>	1.19 (0.09) ab <u>100</u>	1.24 (0.10) a <u>100</u>

	a <u>77</u>						
PCu-2	1.17 (0.11) a	1.03 (0.06) b <u>0</u>	1.26 (0.10) ab <u>2</u>	1.18 (0.08) bc <u>2</u>	1.29 (0.19) a <u>2.5</u>	1.13 (0.08) ab <u>94</u>	
PCu-3	1.11 (0.07) a <u>2</u>	1.04 (0.13) b <u>4</u>	1.17 (0.11) b <u>8</u>	1.24 (0.06) c <u>18</u>	1.10 (0.10) bc <u>2</u>	1.13 (0.07) ab <u>0</u>	
PCu-4	1.13 (0.07) a <u>36</u>	0.94 (0.04) b <u>34</u>	1.10 (0.15) b <u>2</u>	1.00 (0.15) d <u>14</u>	1.01 (0.11) c <u>3</u>	1.03 (0.10) b <u>60</u>	

\* Values represent means of seven replicates per treatment, while figures in parentheses are the standard deviation. Means with a column followed by the same letter are not significantly different using Tukey's Studentized Range Test ( $\alpha = 0.05$ ). Numbers in italics and underline represent the wood failure of the corresponding shear strength, and the unit is percentage (%).